

**Stem Cell Reports, Volume 11**

**Supplemental Information**

***In Vivo* Expansion of Cancer Stemness Affords Novel Cancer Stem Cell**

**Targets: Malignant Rhabdoid Tumor as an Example**

**Hana Golan, Rachel Shukrun, Revital Caspi, Einav Vax, Naomi Pode-Shakked, Sanja Goldberg, Oren Pleniceanu, Dekel D. Bar-Lev, Michal Mark-Danieli, Sara Pritchén, Jasmine Jacob-Hirsch, Itamar Kanter, Ariel Trink, Ginette Schiby, Ron Bilik, Tomer Kalisky, Orit Harari-Steinberg, Amos Toren, and Benjamin Dekel**

## **Supplemental Information**

### ***In-Vivo* Expansion of Cancer Stemness Affords Novel Cancer Stem Cell Targets:**

#### **Malignant Rhabdoid Tumor as an Example**

Hana Golan, Rachel Shukrun, Revital Caspi Einav Vax, Naomi Pode-Shakked, Sanja Goldberg, Oren Pleniceanu, Dekel D. Bar-Lev, Michal Mark Danieli, Sara Pri-Chen, Jasmine Jacob-Hirsch, Itamar Kanter, Ariel Trink, Ginette Schiby, Ron Bilik, Tomer Kalisky, Orit Harari-Steinberg, Amos Toren, Benjamin Dekel

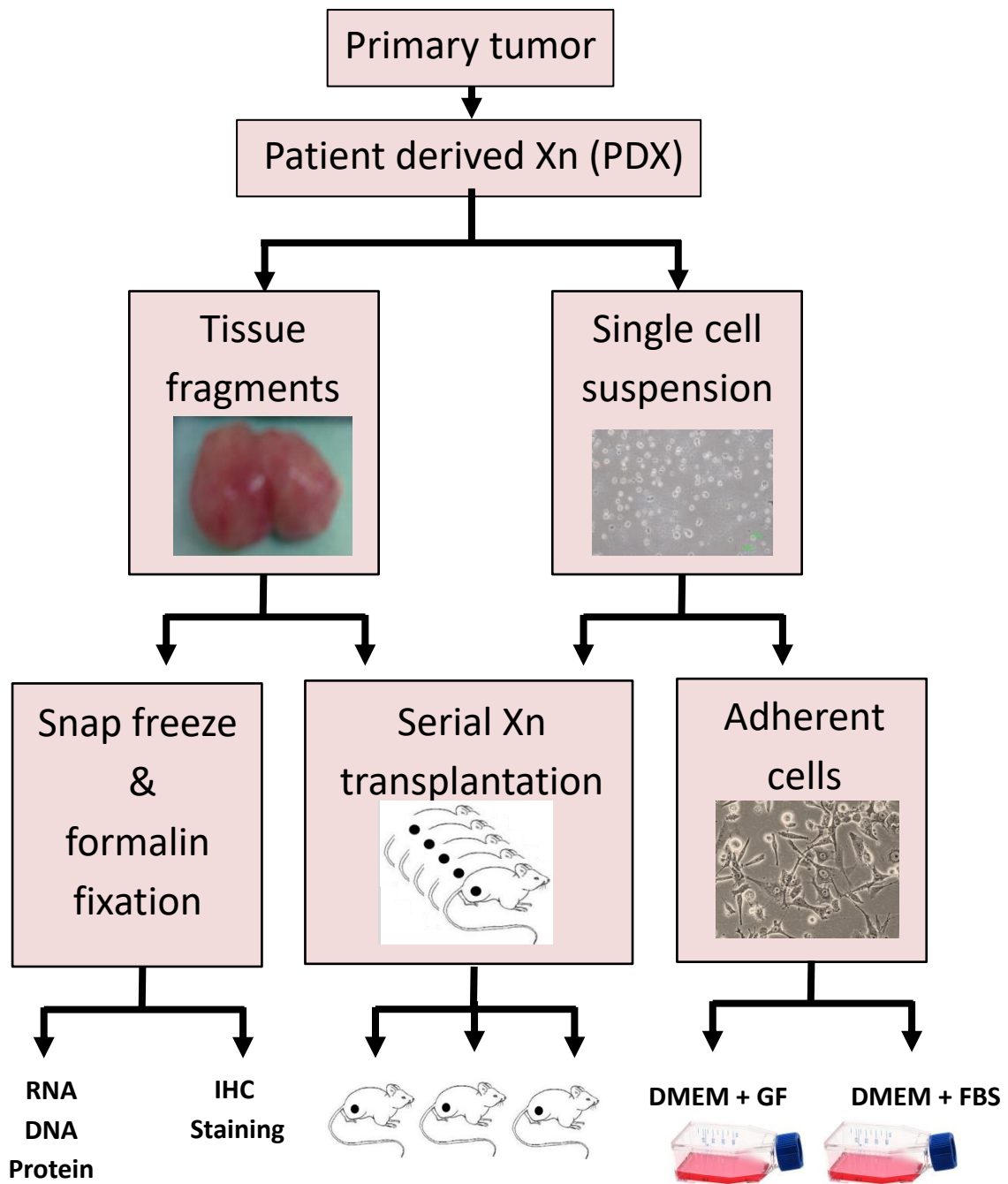


**Figure S1. Establishment of the MRT Xn model (Related to figure 1).** Primary tumor grafts were formed by a subcutaneous transplantation of 2-5 mm tumor pieces into immunodeficient mice. Tumor take was observed in all mice allowing tumor propagation. Sequential propagation of MRT PDX in NOD/SCID mice was performed by tissue samples transplantation or single cell suspensions grafting utilizing a fixed number of  $1 \times 10^6$  cells. Serial propagation allowed us to establish early (<P5), intermediate (P5-P10) and late-passage (P10-P15) MRT PDX. Tissue fragments were also used for IHC staining, RNA, DNA and protein isolation. Adherent cells were also used for in vitro studies of the tumor's cells.

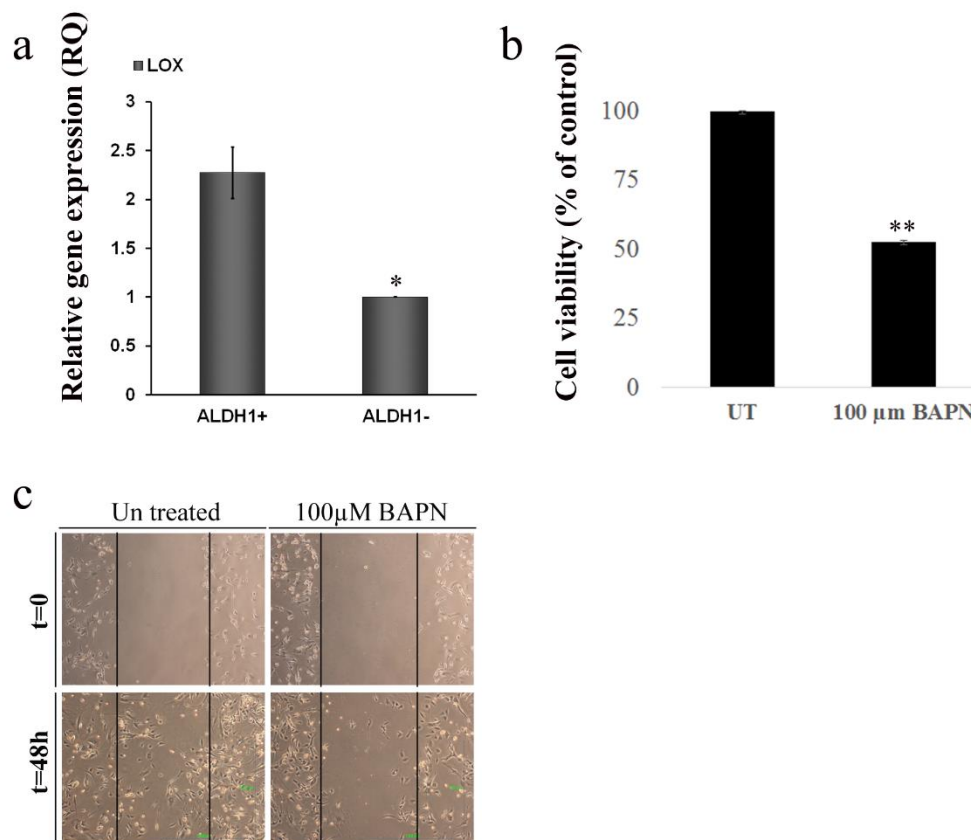


**Figure S2. Functional validation of LOX inhibitor as MRT CIC/CSC therapeutic agent (Related to figures 5-6).** (a) Validation via qRT-PCR revealed high LOX expression in sorted ALDH1+ in comparison to ALDH1- cells. For qRT-PCR analyses the values for ALDH1- cells were used to normalize (therefore=1) and all other values were calculated accordingly. All results are presented as the mean  $\pm$  S.E.M of triplicates on three separated experiments. P values were generated using a 2-tailed unpaired t test \*  $p < 0.05$ ; (b) A MTS analysis, examining cell viability, was performed on PDX-01 (P10) cells grown with different concentration of BAPN (10-1000  $\mu$ M) for 48h. The treatment resulted in significantly reduced proliferation (47% in treated cells in comparison to UT cells) following treatment with 100  $\mu$ M BAPN. All results are presented as the mean  $\pm$  S.E.M of triplicates on three separated experiments \*\*  $p < 0.01$ ; (c) Migration assay revealed that 100  $\mu$ M BAPN treatment for 48h significantly inhibited MRT PDX-01 (P2) cell's migration capacity, as compared to un-treated cells. Scale bar, 1000  $\mu$ m.

**Table S1. Generation and establishment of human MRT PDX model in NOD/SCID mice (Related to figure 1 and figure S1)**

Passage	Cells Injections*			Tissue transplantations		
	No. of injections	No. of tumors engrafted	(%) engraftment	No. of transplantations	No. of tissue engrafted	(%) engraftment
P1	0	0	-	4	4	100
P2	6	4	67	8	8	100
P3	12	10	83	14	13	93
P4	8	7	88	6	6	100
P5	8	8	100	4	3	75
P6	4	4	100	6	4	67
P7	2	2	100	4	2	50
P8	4	2	50	2	1	50
P9	4	4	100	0	0	-
P10	2	2	100	0	0	-
P11	4	4	100	2	2	100
P12	2	2	100	2	2	100
P13	4	4	100	2	2	100
P14	4	4	100	2	2	100
P15	4	4	100	1	1	100
P16	4	4	100	0	0	-
Total	72	65	90	57	50	88

Generation of primary human MRT PDX from serial  $1 \times 10^6$ \* cell injections and tissue transplantations (Obtained from MRT-01).

**Table S2. MRT PDX frequency and characteristics during propagation (Related to figure 1 and figure S1)**

Passage		Engraftment rate (%)	Days to engraftment (mean)*	PDX weight/days to resection ratio (mean)**
Early	P2	4/6	34	0.04
	P3	10/12	23	0.07
	P4	7/8	24	0.08
		<b>21/26 (80)</b>	<b>26</b>	<b>0.06</b>
Intermediate	P5	8/8	15	0.11
	P6	4/4	22	0.09
	P7	2/2	15	0.12
	P8	2/4	28	0.10
	P9	4/4	23	0.06
	P10	2/2	22	0.06
		<b>22/24 (92)</b>	<b>20</b>	<b>0.09</b>
Late	P11	4/4	19	0.05
	P12	2/2	20	0.12
	P13	4/4	16	0.08
	P14	4/4	16	0.11
	P15	4/4	14	0.19
	P16	4/4	14	0.16
		<b>22/22 (100)</b>	<b>16</b>	<b>0.12</b>

Table summarizing the frequency and characteristics of secondary tumor formation from  $1 \times 10^6$  cells obtained from MRT-01 PDX and further propagated. During serial propagation of MRT PDX shorter time to tumor engraftment and accelerated tumor growth were noticed. In the comparison between early and late PDX passages \* $p < 0.001$  \*\*  $p = 0.003$ , Mann-Whitney test. Results are presented as the mean of pooled data from early, intermediate and late passages.

**Table S3: Limiting dilution xenotransplantation summary representing PDX CSC frequency during propagation (Related to figure 1 and figure S1)**

Number of Injected Tumor Cells	Number of grafted tumors/ number of injections		
	Early	Intermediate	Late
1000	1/10	4/8	9/10
750	-	1/2	2/2
500	2/10	2/3	3/5
250	-	-	2/2
100	1/16	-	6/8
50	0/4	-	1/2
Tumor propagating cell frequency (95% CI)*	<b>1/3930</b> (10628, 1453)	<b>1/1107</b> (2392, 512)	<b>1/252</b> (453, 151)

Summary of CSC frequency estimated by limiting dilution xenotransplantation of cells isolated from early, intermediate and late PDX passages (Obtained from MRT-01). The data are presented as the ratio of injections that formed tumors within 12 weeks. Bold numbers represent the estimated CSC frequency. In the comparison between low and high PDX passages \*p<0.001, Chi-square test.

**Table S4. 50 most upregulated differentially expressed genes between Primary tumor (P) and PDX ( Related to figure 2)**

Gene Symbol	Description	Fold-Change		
		P2 > P	P7 > P	P17 > P
Fold change > 2, p < .05				
<i>CXCL6</i>	Chemokine (C-X-C motif) ligand 6	12.22	119.43	287.01
<i>CXCL5</i>	Chemokine (C-X-C motif) ligand 5	12.12	55.80	246.76
<i>SEMA3C</i>	Sema domain, (semaphorin) 3C	54.99	105.18	235.41
<i>GPM6A</i>	Glycoprotein M6A	28.48	120.72	169.37
<i>FSTL5</i>	Follistatin-like 5	10.22	110.78	139.89
<i>ALDH1A1</i>	Aldehyde dehydrogenase 1 family, member A1	23.67	100.75	130.37
<i>ANXA1</i>	Annexin A1	41.88	63.26	115.01
<i>LOX</i>	Lysyl oxidase	32.48	25.39	109.51
<i>DSEL</i>	Dermatan sulfate epimerase-like	13.96	38.63	97.57
<i>DLX2</i>	Distal-less homeobox 2	5.68	4.63	75.98
<i>TSPAN12</i>	Tetraspanin 12	22.75	30.78	70.46
<i>CXCL1</i>	Chemokine (C-X-C motif) ligand 1	2.71	31.51	62.47
<i>SCN9A</i>	Sodium channel, voltage-gated, type IX, alpha subunit	12.01	10.61	59.95
<i>MAP2</i>	Microtubule-associated protein 2	9.53	42.35	53.25
<i>DST</i>	Dystonin	7.31	19.55	52.11
<i>MSX2</i>	Msh homeobox 2	2.72	2.22	45.57
<i>DKK1</i>	Dickkopf homolog 1 ( <i>Xenopus laevis</i> )	13.31	13.38	44.42
<i>CHN1</i>	Chimerin (chimaerin) 1	2.35	22.61	43.43
<i>DIRAS3</i>	DIRAS family, GTP-binding RAS-like 3	15.40	18.69	42.04
<i>HGF</i>	Hepatocyte growth factor (hepapoietin A; scatter factor)	17.16	13.83	39.54
<i>DLX1</i>	Distal-less homeobox 1	3.60	4.83	37.81
<i>THBS2</i>	Thrombospondin 2	2.65	2.25	37.41
<i>HMCN1</i>	Hemicentin 1	14.24	17.17	37.11
<i>PDGFC</i>	Platelet derived growth factor C	4.40	5.47	35.51
<i>ELMOD1</i>	ELMO/CED-12 domain containing 1	4.17	21.90	35.41
<i>TFAP2A</i>	Transcription factor AP-2 alpha	19.33	4.06	33.27
<i>GABRA2</i>	Gamma-aminobutyric acid (GABA) A receptor, alpha 2	6.63	2.93	33.01
<i>COL11A1</i>	Collagen, type XI, alpha 1	14.51	14.43	32.05
<i>MYCN</i>	V-myc myelocytomatosis viral related oncogene	2.56	2.87	31.32
<i>QPRT</i>	Quinolinate phosphoribosyltransferase	11.38	13.47	29.88
<i>TSPAN8</i>	Tetraspanin 8	2.59	20.83	29.04
<i>EPHA3</i>	EPH receptor A3	7.85	20.24	28.91
<i>IFI44L</i>	Interferon-induced protein 44-like	10.18	7.32	25.87
<i>SMC4</i>	Structural maintenance of chromosomes 4	14.23	21.54	25.09
<i>PCDH7</i>	Protocadherin 7	8.03	20.17	24.67
<i>CADM2</i>	Cell adhesion molecule 2	8.51	20.82	24.64
<i>UACA</i>	Uveal autoantigen with coiled-coil domains and ankyrin repeats	9.41	16.04	23.98
<i>STAU2</i>	Staufen, RNA binding protein, homolog 2 ( <i>Drosophila</i> )	3.49	4.62	23.88



<i>ARHGAP29</i>	Rho GTPase activating protein 29	3.22	11.44	22.46
<i>FLRT2</i>	Fibronectin leucine rich transmembrane protein 2	7.70	21.07	21.83
<i>LIPG</i>	Lipase, endothelial	4.91	6.94	21.60
<i>PLOD2</i>	Procollagen-lysine, 2-oxoglutarate 5-dioxygenase 2	8.42	8.50	20.98
<i>COL12A1</i>	Collagen, type XII, alpha 1	5.17	2.21	20.84
<i>DEPDC1</i>	DEP domain containing 1	10.10	14.37	20.65
<i>MST4</i>	Serine/threonine protein kinase MST4	2.85	7.99	20.05
<i>PCDH9</i>	Protocadherin 9	7.71	10.56	19.68
<i>GGH</i>	Gamma-glutamyl hydrolase	5.68	7.75	18.92
<i>SLC35F2</i>	Solute carrier family 35, member F2	6.15	12.23	18.92
<i>FGF2</i>	Fibroblast growth factor 2 (basic)	9.56	7.19	18.34
<i>SLC4A7</i>	Solute carrier family 4, sodium bicarbonate cotransporter, member 7	4.87	14.20	16.36

**Table S5. 50 most downregulated differentially expressed genes between Primary tumor (P) and PDX ( Related to figure 2)**

Gene Symbol	Description	Fold-Change		
		P2 > P	P7> P	P17> P
Fold change > 2, p < .05				
<i>HBG1</i>	Hemoglobin, gamma A	-363.05	-381.27	-433.42
<i>HBB</i>	Hemoglobin, beta	-354.41	-291.87	-425.64
<i>SPP1</i>	Secreted phosphoprotein 1	-139.51	-20.33	-190.68
<i>FIBIN</i>	Fin bud initiation factor homolog (zebrafish)	-3.52	-3.31	-138.71
<i>GLUL</i>	Glutamate-ammonia ligase	-12.60	-32.40	-119.90
<i>HBG1</i>	Hemoglobin, gamma A /// hemoglobin, gamma G	-142.99	-151.48	-105.34
<i>CD163</i>	CD163 molecule	-87.44	-96.26	-102.49
<i>CCL4</i>	Chemokine (C-C motif) ligand 4	-91.45	-82.14	-92.12
<i>RNASE1</i>	Ribonuclease, rnase A family, 1 (pancreatic)	-69.72	-86.54	-82.32
<i>C1QB</i>	Complement component 1, q subcomponent, B chain	-98.58	-88.44	-82.31
<i>COL4A1</i>	Collagen, type IV, alpha 1	-62.38	-61.76	-76.29
<i>HLA-DRA</i>	Major histocompatibility complex, class II, DR alpha	-60.00	-45.47	-69.08
<i>SERPIN2</i>	Serpin peptidase inhibitor, clade B (ovalbumin), member 2	-4.38	-82.31	-68.87
<i>SSTR1</i>	Somatostatin receptor 1	-6.70	-8.13	-68.45
<i>SRGN</i>	Serglycin	-5.32	-4.12	-65.45
<i>SHISA2</i>	Shisa homolog 2 ( <i>Xenopus laevis</i> )	-3.79	-7.83	-64.46
<i>AGR2</i>	Anterior gradient homolog 2 ( <i>Xenopus laevis</i> )	-44.20	-58.88	-63.35
<i>FCGR3A</i>	Fc fragment of igg, low affinity iiii, receptor (CD16a)	-56.29	-60.65	-62.06
<i>COL4A2</i>	Collagen, type IV, alpha 2	-19.45	-26.18	-60.92
<i>IGFBP7</i>	Insulin-like growth factor binding protein 7	-2.32	-5.09	-54.40
<i>NKX3-2</i>	NK3 homeobox 2	-27.78	-50.59	-53.67
<i>LAPTM5</i>	Lysosomal protein transmembrane 5	-50.98	-48.79	-50.81
<i>HLA-DOA</i>	Major histocompatibility complex, class II, DO alpha	-2.82	-2.28	-46.24
<i>S100A9</i>	S100 calcium binding protein A9	-27.34	-39.34	-42.01
<i>CD14</i>	CD14 molecule	-30.95	-42.85	-41.24
<i>F13A1</i>	Coagulation factor XIII, A1 polypeptide	-39.68	-38.36	-38.51
<i>PAPPA</i>	Pregnancy-associated plasma protein A, pappalysin 1	-6.74	-44.51	-37.74
<i>VSIG4</i>	V-set and immunoglobulin domain containing 4	-46.99	-33.11	-36.15
<i>LIN28A</i>	Lin-28 homolog A ( <i>C. Elegans</i> )	-32.23	-30.30	-34.50
<i>VWF</i>	Von Willebrand factor	-33.17	-29.05	-34.40
<i>MS4A6A</i>	Membrane-spanning 4-domains, subfamily A, member 6A	-40.03	-33.79	-34.10
<i>LPPR5</i>	Lipid phosphate phosphatase-related protein type 5	-8.92	-19.85	-33.22
<i>LCPI</i>	Lymphocyte cytosolic protein 1 (L-plastin)	-29.95	-28.62	-30.75
<i>FOXA1</i>	Forkhead box A1	-19.12	-14.49	-30.28
<i>KLK8 /// KLK9</i>	Kallikrein-related peptidase 8 /// kallikrein-related peptidase 9	-7.17	-12.94	-29.52
<i>LYZ</i>	Lysozyme	-29.93	-27.82	-29.41

<i>HBA1 /// HBA2</i>	Hemoglobin, alpha 1 /// hemoglobin, alpha 2	-31.16	-31.23	-29.08
<i>HLA-DPA1</i>	Major histocompatibility complex, class II, DP alpha 1	-11.24	-12.77	-27.20
<i>PALMD</i>	Palmdelphin	-3.88	-12.57	-26.73
<i>IFI30</i>	Interferon, gamma-inducible protein 30	-11.03	-23.08	-25.83
<i>IFI27</i>	Interferon, alpha-inducible protein 27	-10.11	-27.07	-25.18
<i>ROBO4</i>	Roundabout homolog 4, magic roundabout (Drosophila)	-18.14	-13.24	-24.28
<i>A2M</i>	Alpha-2-macroglobulin	-26.60	-27.28	-24.08
<i>CD93</i>	CD93 molecule	-21.54	-22.65	-23.81
<i>C1orf130</i>	Chromosome 1 open reading frame 130	-11.32	-24.20	-23.55
<i>HLA-DRB1//B3//B4//B5</i>	Major histocompatibility complex, class II, DR beta 1 /// major histocompatibility comp	-11.78	-14.92	-22.99
<i>TMEM158</i>	Transmembrane protein 158 (gene/pseudogene)	-4.43	-15.32	-21.48
<i>MAFB</i>	V-maf musculoaponeurotic fibrosarcoma oncogene homolog B (avian)	-7.70	-18.33	-21.12
<i>DPPA4</i>	Developmental pluripotency associated 4	-14.92	-21.80	-20.98
<i>LYVE1</i>	Lymphatic vessel endothelial hyaluronan receptor 1	-22.29	-20.61	-20.80

## Supplemental Experimental Procedures

### Immunohistochemical staining of primary MRT and MRT PDX.

Immunostainings were performed as previously described (Dekel et al., 2006b). For H&E staining slides were incubated in Mayer's Hematoxylin solution (Sigma-Aldrich) followed by incubation in Eosin (Sigma-Aldrich). Anti-human ALDH1 antibody (BD Biosciences, #611195) was used at a dilution of 1:100. Anti-human LOX antibody (Novous, nb 100-2527) was used at a dilution of 1:200. The immunoreaction was visualized by an HRP-based chromogen/substrate system (liquid DAB substrate kit – Zymed, San Francisco, CA, USA). All Sections were stained for Vimentin, EMA, SMA, AE1/AE3, NFP and INI1 using conventional immunohistochemical procedures. (Dekel et al., 2006b) All antibody dilutions were carried out as recommended by the manufacturers of the staining antibodies. Images were produced using Olympus BX51TF.

### Fluorescence-activated cell sorting (FACS) analysis

FACS analysis of primary MRT cells and fresh PDX derived cells was performed as previously described (Pode-Shakked et al., 2013). The following primary antibodies were used: CD24 (eBioscience, 120247-42), CD34 (Miltenyi, 3008100), CD56 (eBioscience, 1205942), CD90 (Beckman Coulter, IM3600U) and 7AAD;( eBioscience, San Diego, CA). Detection of cells with high ALDH1 enzymatic activity was performed using the ALDEFLUOR kit (StemCell Technologies, Durham, NC, USA). FACS sorting according to ALDH1 activity was performed as previously described (Pode-Shakked et al., 2013).

### qRT-PCR analysis

Quantitative reverse transcription PCR (qRT-PCR) was carried out to determine fold changes in expression of a selection of genes as previously described (Pode-Shakked et al., 2013). Statistical analysis was performed using a non-paired 2-tails T-test. Statistical significance was considered at  $P < 0.05$ . All results are presented as the mean  $\pm$  S.E.M of triplicates on three separated experiments.

### Microarray

The microarray data is deposited in publicly library (GEO); accession numbers GSE7269. All experiments were performed using Affymetrix HU GENE1.0st oligonucleotide arrays. Total RNA from each sample was used to prepare biotinylated target cDNA, according to the manufacturer's recommendations. The target cDNA generated from each sample was processed as per manufacturer's recommendation using an Affymetrix Gene Chip Instrument System. Details of quality control measures can be found online. Significantly changed genes were filtered as changed by at least twofold (p-value: 0.05).

### RNA sequencing analysis

The RNA sequencing data is deposited in publicly library (GEO); accession numbers GSE114471. Bulk total RNA was prepared from  $\sim 1.5 \times 10^5$  cells using the Direct-zol™-96 RNA Isolation kit (Zymo Research) according to the manufacturer's instructions and stored in  $-80^\circ\text{C}$  in nuclease free water. Total RNA was quantified on an Agilent BioAnalyzer and 1  $\mu\text{g}$  of RNA was used to prepare cDNA libraries using the TruSeq mRNA-Seq library protocol (Illumina). Libraries were sequenced 1  $\times$  50 bases on an Illumina HiSeq 2000 machine in two lanes. Data from the high throughput sequencing was analyzed base on the protocol by Anders et al (Anders et al., 2013).

### Genetic Cell Labeling

To establish genetically marked MRT-PDX cells, HEK293 cells were initially transformed. HEK293 cells were maintained in DMEM supplemented with 10% fetal calf serum, l-glutamine, penicillin, and streptomycin (Biological Industries, Beit-Ha'emek, Israel), at  $37^\circ\text{C}$  in a 5%  $\text{CO}_2$ -enriched atmosphere. Cells were transfected using calcium phosphate with three lentiviral vectors: 7.5  $\mu\text{g}$  pHR-CMV-mCherry, 5  $\mu\text{g}$   $\Delta\text{R8.2}$ , and 2.5  $\mu\text{g}$  pMD2. G. After 6 hours, the supernatants were replaced with 5 mL of fresh medium. Supernatants of transfected cells were supplemented with HEPES (pH 7.0; 50 mmol/L final concentration) and filtered through a 0.45- $\mu\text{m}$  pore-size filter; 2 mL was placed on the targeted cells for 2 hours with the addition of 8  $\mu\text{g}/\text{mL}$  Polybrene (hexadimethrine bromide; Sigma-Aldrich), and then 3 mL of fresh medium was added. These viral-like particles were used to infect MRT-PDX cells (2  $\times$  10<sup>5</sup> cells in 60-mm-diameter dishes). Expression of the mCherry reporter gene was analyzed at 2 days after infection.

## Supplemental References

Anders, S., McCarthy, D.J., Chen, Y., Okoniewski, M., Smyth, G.K., Huber, W., and Robinson, M.D. (2013). Count-based differential expression analysis of RNA sequencing data using R and Bioconductor. *Nature protocols* 8, 1765-1786.

Dekel, B., Zangi, L., Shezen, E., Reich-Zeliger, S., Eventov-Friedman, S., Katchman, H., Jacob-Hirsch, J., Amariglio, N., Rechavi, G., Margalit, R., et al. (2006b). Isolation and characterization of nontubular sca-1+lin- multipotent stem/progenitor cells from adult mouse kidney. *J Am Soc Nephrol* 17, 3300-3314.

Pode-Shakked, N., Shukrun, R., Mark-Danieli, M., Tsvetkov, P., Bahar, S., Pri-Chen, S., Goldstein, R.S., Rom-Gross, E., Mor, Y., Fridman, E., *et al.* (2013). The isolation and characterization of renal cancer initiating cells from human Wilms' tumour xenografts unveils new therapeutic targets. *EMBO molecular medicine* 5, 18-37.